Memoirs of the Faculty of Science, Kyoto University, Series of Physics, Astrophysics, Geophysics and Chemistry, Vol. XXXIII, No. 3. Article 3, 1971.

THREE-ALPHA-DECAY MECHANISM OF HIGHER EXCITED STATES OF ^{12}C IN THE REACTION $^{11}B(p, 3\alpha)$

By

Isao YAMANE

Department of Physics, Faculty of Science, Kyoto University, Kyoto, Japan

(Received September 26, 1970)

SYNOPSIS

The three-α-decay mechanism of higher excited states of ^{12}C is investigated in the reaction $^{11}B(p, 3\alpha)$ to obtain information about the structure of those states. Coincidence measurements are carried out under the detection condition devised to distinguish between the sequential decay and the direct three α decay. Dependences of energy spectra of coincident α particles upon the incident energy and the angle are measured between 138 keV and 232 keV and between 2.00 MeV and 5.30 MeV of the incident energy. The spectra show strong dependence upon the resonances. At the 163 keV (16.11 MeV in ^{12}C; 2^+, T=1), the 2.62 MeV (18.36 MeV; 3^-, T=0), the 3.75 MeV (19.4 MeV; 2^+, T=0) and the 5.10 MeV (20.64 MeV; 3^-, T=1) resonances the spectra suggest the direct three α decay. Around 215 keV and 2.4 MeV, and at the 3.5 MeV (19.2 MeV; 1^-, T=1) and the 4.92 MeV (20.47 MeV) resonances, they suggest the sequential decay. The direct-three-α-decay states are considered to have some "α cluster structures".

1. Introduction

For the very light nuclei of mass numbers $A \leqq 12$, some evidences for the cluster structures have been discussed,[1] and such structures have been investigated both theoretically[2] and experimentally.[3]

Recently it becomes clear that there are cluster or quasimolecular states in the region of medium and high excitation in light nuclei.[4] In the same region, there appear some characteristic states such as the giant resonance states[5] and the isobaric analogue states,[6] and etc. These states and many other states that appear in the region are usually considered to have structures based on the single particle excitation. On the other hand, the cluster or quasi-molecular states have structures based on the many particle correlation. Therefore, the investigation on the cluster or quasi-molecular states is significant to make clear the existence of a new mode of nuclear structure.

The main method used to find the cluster state is to compare the particle reduced width measured by the experiment with the Wigner-limit. As long as two body reaction is concerned, this method is very useful. However, when three or more particles come out in the final state of the reaction, the meaning of the reduced width of a particle is not so clear as in the two body reaction.[7] Such a reaction often occurs associated with the medium and high excited

states of light nuclei. In particular, states of ^{9}Be or ^{12}C excited higher than several MeV, in many case, decay to three particles. In these cases, it is very important to decide the reaction mechanism, because the three-body-decay mechanism is considered to reflect the structure of the decaying states.

In this work, the mechanism of the three α decay is investigated to obtain informations about the structure of the higher excited states of ^{12}C formed in the reaction $^{11}B+p$.

Many investigations on the reaction $^{11}B+p$ have been worked with the method detecting only one outgoing particle for the open channels shown in Fig. 1. It is remarkable that compound states of ^{12}C formed at lower incident energies have appreciably large α-particle reduced widths. In particular, the α decay of such states is strongly enhanced in the α_1 channel, provided that the α decay proceeds sequentially through states of ^{8}Be.

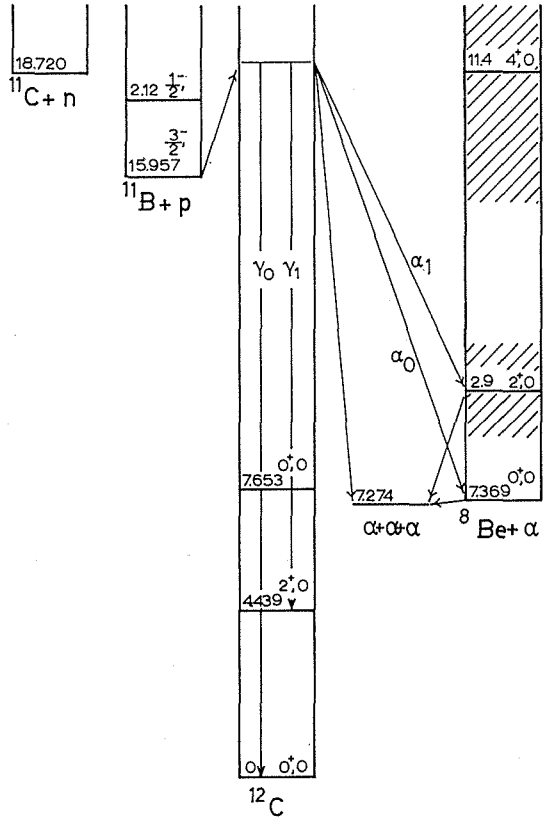

Fig. 1. Energy-level diagram for the reactions of the type $^{11}B(p, x)Y$.

However, it is not so clearly decided whether the α decay proceeds sequentially or not. This is partly because the width of the first excited state of ^{8}Be is as large as large as 1.5 MeV,[8] and partly because the energy of α_1 just overlap those of α particles that are made from breakup of the residual ^{8}Be* (1st). They are called α_{11} and α_{12} hereafter. So, even if the α decay of ^{12}C proceeds only sequentially, the energy spectrum of α_1 is masked in the con-

tinuum spectrum and detailed informations are not obtained for the α_1 channel. Moreover, it changes the shape corresponding to the level of ^{12}C, because the yield ratio of α_1 and α_{11} (or α_{12}) in a solid angle changes depending on the α_1 angular distribution.

As long as one adopts the method to measure the spectrum of only one outgoing particle, one cannot exclude the possibility of the mechanism of the direct three α decay. When the compound state of ^{12}C decays directly to three α particles, the energy spectrum of α particles has the statistical shape and makes a continuum spectrum. The observed spectrum is complicated due to the coexistence of the sequential and the direct three-α-decay mechanism.

There are some theoretical works which argue the shape of the α energy spectrum from the viewpoint of the sequential decay.[9] However, it is difficult to discuss successfully the decay mechanism without determining all kinematical parameters of the final three α state by means of the coincidence technique.[10,11]

The development of the solid state detector and the multichannel pulse height analyzer made it possible to investigate the decay mechanism by the measurement of the energy spectrum of coincident α particles. Followinge to the first work by D. Dehnhard et al.,[11] some experiments have been worked on the α decay mechanism at some excitation energies of ^{12}C between 16 MeV $\leqq E_x \leqq$ 23 MeV. These are classified into three groups by their standpoints; the Marburg group,[11,12] the Rice Group[13,14] and the group which include many other investigators represented by those of France.[15~17]

D. Dehnhard et al.[11] discoverved some anomalies in the shapes of the coincidence energy spectra of α particles from the 16.11 MeV state of ^{12}C which corresponds to the 163 keV resonance. Those anomalies were not explained by the simple sequential decay mechanism, then Marburg group attributed them to the direct three α decay. At some energies of incident proton near to 163 keV[11] and at 675 keV,[12] they detected two α particles with coindicence method. They measured the single dimensional energy spectrum of coincident α particles. They found that at the 163 keV resonance the spectra showed only one broad peak. Such a peak could not be explained by the sequential decay mechanism. However, at 150 keV spectra show two separated peaks expected from the sequential decay mechanism. Later, they measured the same spectra at the 675 keV resonance[12] and confiirmed separated peaks of the sequential decay mechansim. They discuss their results by the Dalitz diagram method on the base of the "generalized angular momentum theory".[18,19]

The Rice group, from the standpoint of the sequential decay mechanism, tried to explain the energy spectra of coincident α particles on the "generalized density of states theory."[20] In their experiment, proton beams of several energies (E_p=2.0, 2.65, 3.25, 3.75, 4.0, 5.08, 5.64 MeV[13]; E_p=163 keV[14]), were bombarded to the ^{11}B target, and two dimensional energy spectra of coincident α particles were measured. Obtained spectra show one or two peaks, along the kinematical loci which are expected from the sequestial decay mechanism. These spectra are very likely to show the shapes expected from the sequential decay mechanism, except some large distortions. To explain those distortions of spectra, they introduced some interference effects.[21] They concluded that the contribution from the direct three α decay cannot be greater than five percent of the total yield and is probably much smaller in the cases of E_p=2.0 ~5.64 MeV,[13] and that it can be estimated at less than a few percent of the

sequential decay in the case of the 163 keV resonance.[14]

The last group also adopt the sequential decay mechanism. Their main aims of investigation are to compare their formalism to the experimental data[17] or to find other selection rules for three body decay from energy spectra of coincident α particles.[16]

As abovementioned, it is considered that compound states of ^{12}C formed by the reaction $^{11}B+p$ decay to three α particles mainly through the sequential decay process, with the exceptional case of the 16.11 MeV state.

However those conclusions mentioned above do not describe the whole features of the three α decay, because the detecting conditions of previous measurements are not sufficient to get suitable data for the problem and also because dependence of the spectra on the incident energy is not measured. Therefore, it is worthwhile to seach for the possibility of the direct three α decay from other states of ^{12}C than the 16.11 MeV state.

In order to make clear the sequential decay mechanism, it is necessary to measure the energy spectrum of coincident α particles under the condition that peaks of α_1 and α_{11} (or α_{12}) are separated from each other sufficiently. On the other hand, in order to make clear the direct three-α-decay mechanism, it is necessary to do under the condition that relative energies of all pairs of α particles are high over a sufficiently wide region in the spectrum. Those relative energies should be at least higher than the energy to form the first excited state of ^8Be. When the relative energy becomes lower than that energy, the final state interaction probably affects the pair of α particles, and the shape of the spectrum will deviate from that of the statistical distribution. These condititions must be simultaneously satisfied to clarify the decay mechanism.

Furthermore it is worthwhile noting that the previous measurements are limited only at some energies of incident proton and energy dependence of the spectrum of coincident α particles is not measured. So much attention is not paid to the change of the shape of the spectrum depending on the incident energy. One reason is that the problem to decide the decay mechanism is treated not so strongly correlated to the investigation of the structure of the decaying state.

The main aim of the prevent works is to obtain informations about the structure of higher excited states of ^{12}C, which are considered to be closely related with the decay mechanism of those states. So the experiment is planned to measure the dependence of the energy spectrum of coincident α particles on the incident proton energy. The measurements are performed so as to satisfy simultaneously the condition for the sequential decay mechanism and the condition for the direct three-α-decay mechanism. The Cockcroft-Walton accelerator and the tandem Van de Graaff acclerator in the Department of Physics, Kyoto University are used. The energy regions of the experiments are from 138 keV to 232 keV and from 2.00 MeV to 5.30 MeV in the incident proton energy.

In this paper, a large portion of description is devoted to the process to decide the mechanism of the three α decay. In the next section, there are discussed what sort of measurement are desirable to decide the mechanism of the three α decay from the kinematical and dynamical relations of the reaction. In the section 3 the experimental procedures are described and in the section 4 the results are described. The results show strong dependence of the spectrum on the incident energy. They are discussed with respect to the decay mecha-

anism and the structure of the decaying states in the section 5. It is shown that the mechanism of the direct three α decay should be considered for some resonances. In the section 6, conclusions derived from this work are listed.

2. Reaction Kinematics and Dynamics

2.1 Kinematics

On the kinematical relations in the nuclear reaction of the type A+B→C+D+E, many detailed descriptions have been published, so here are only mentioned some important points. The more complete description is given in ref. 22).

At first, it is shown that the three particle system is completely determined by the coincidence measurement. The kinematical condition of the three particle system is determined by giving the laboratory momenta $\boldsymbol{p}_1$, $\boldsymbol{p}_2$ and $\boldsymbol{p}_3$ of the three particles. These nine degrees of freedom are reduced to five by the four conservation laws, as follows;

$$\boldsymbol{p}_1+\boldsymbol{p}_2+\boldsymbol{p}_3=\boldsymbol{P}_0, \tag{1}$$

$$\boldsymbol{E}_1+\boldsymbol{E}_2+\boldsymbol{E}_3=\boldsymbol{E}_0+\boldsymbol{Q}, \tag{2}$$

where $\boldsymbol{P}_0$ and E_0 ane the momentum and the kinetic energy of the projectile in the laboratory system, E_1, E_2 and E_3 are the kinetic energies of the final three particles in the laboratory system, and Q is the Q-value of the reaction. The residual five parameters are never fully determined by detecting only one particle.

On the other hand, they are fully determined, when two of the final three particles are detected with the coincidence method. When the momenta of three particles in the center of mass system are denoted by $\boldsymbol{p}_1^c$, $\boldsymbol{p}_2^c$ and $\boldsymbol{p}_3^c$, then $\boldsymbol{p}_1^c+\boldsymbol{p}_2^c+\boldsymbol{p}_3^c=0$ and the number of the degree of freedom is reduced to six. These

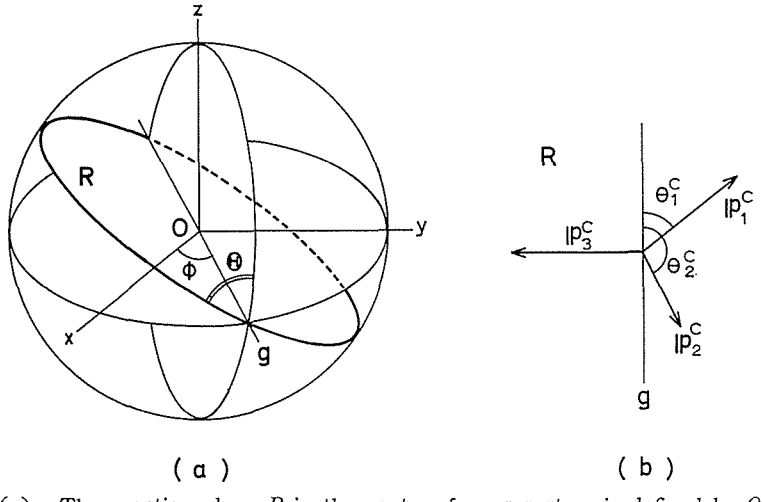

Fig. 2(a). The reaction plane R in the center-of-mass system is defined by Θ and ϕ.
2(b). The final state in R is defined, for example, by θ_1^c, θ_2^c and magnetude of one of three momenta p_1^c, p_2^c and p_3^c by means of the conservation low of energy.

three momenta are kept in a plane, the reaction plane, which is called $\boldsymbol{R}$ hereafter. Thus the residual six degrees of freedom can be separated into those concerned with the plane R and those concerned with motions of the three particles in R. Two independent variables are necessary to determine R. Actually when we assume the coordinate system O-xyz in the center of mass system as is shown in Fig. 2(a), and denote the intersection of R and the plane x-O-y as g, then the position of R is determined by the angle Θ between R and the plane z-O-g, and the angle ϕ between g and O-x. Motion of the particles in R is determined by a suitable set of four independent variables, for example θ_1^c (the angle between $\boldsymbol{p}_1^c$ and g), θ_2^c (the angle between $\boldsymbol{p}_2^c$ and g), p_1^c (the magnitude of the momentum $\boldsymbol{p}_1^c$) and p_2^c (the magnitude of the momentum $\boldsymbol{p}_2^c$). However, the energy conservation law reduces the four independent variables to three.

In the coincidence measurement two detectors are used, so the four angles Θ, ϕ, θ_1^c and θ_2^c are always determined by the condition of the detector arrangement. Thus, if p_1^c or the energy E_1 of particle 1 is measured with the coincidence method, the final state is uniquely determined. Actually, not only the energy of the particle 1 but also the energy of the particle 2 are often measured in coincidence. Although being over-measurement, this method is particularly useful both for precise particle identification and for reduction of the background.

In present experiments energies of two α particles are measured in coincidence and two dimensional energy spectra are obtained. The relation of the energies of two α particles is given;

$$\begin{aligned}&\frac{1}{m_3}\left[E_1(m_1+m_3)+E_2(m_2+m_3)-2(m_0m_1E_0E_1)^{1/2}\cos\theta_1\right.\\&\left.-2(m_0m_2E_0E_2)^{1/2}\cos\theta_2+2(m_1m_2E_1E_2)^{1/2}\cos\theta_{12}\right]\\&=Q+E_0\left(1-\frac{m_0}{m_3}\right),\end{aligned}\tag{3}$$

where

$$\cos\theta_{12}=\cos\theta_1\cos\theta_2+\sin\theta_1\sin\theta_2\cdot\cos(\phi_1-\phi_2).$$

E_i and m_i represent the kinetic energy and the mass of the particle i. θ_i and ϕ_i represent the polar and the azimutal angle of emission of the particle i with respect to the direction of the incident beam in the laboratory system. The subscript 0 indicates the projectile, 1 and 2 indicate the particles which are detected by the detectors 1 and 2, and 3 indicates the undetected particle. Eq. (3) describes such a locus for each set of θ_1 and θ_2 as is shown in Fig. 3(a). Each point on the locus corresponds one by one to a final state. The relative energy E_{23} between particles 2 and 3 is given

$$E_{23}=E_{to\,t}^c-\frac{m_1+m_2+m_3}{m_2+m_3}E_1^c,\tag{4}$$

where

$$E_{to\,t}^c=Q+\frac{m_t}{m_0+m_t}E_0,$$
$$E_1^c=\left[(E_1)^{1/2}-a_1\cos\theta_1\right]^2+(a_1)^2\sin^2\theta_1,$$

and

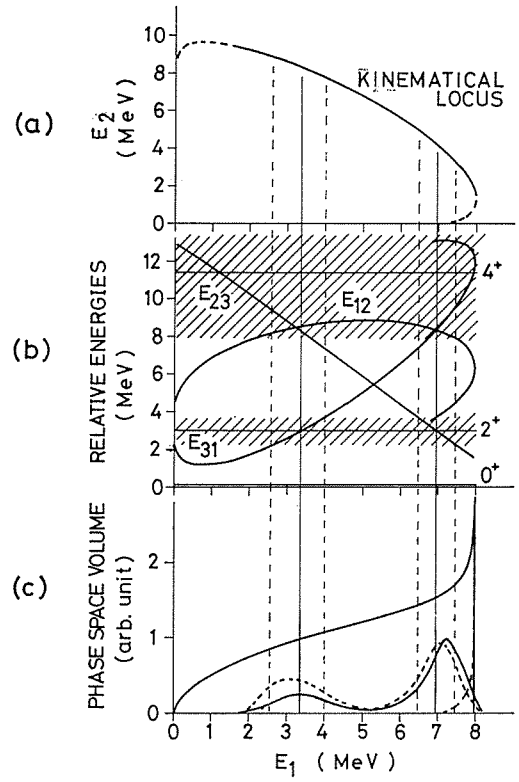

Fig. 3. Kinematical relations. (a) The kinematical locus of energies of two detected particles in the laboratory system. Parts of the broken line are cut off by the discriminators. (b) Relative energy to E_1 curves and energy levels of ^8Be. E_{ij} indicates the relative energy of particles i and j. Horizontal lines indicate centers of energy levels of ^8Be. Shaded bands indicate FWHM's of each level. Vertical solid lines indicate energies of E_1 at which curves of relative energy intersect with the horizontal line of the firt excited state of ^8Be. Widths between vertical broken lines correspond to the FWHM of the first excited state of ^8Be. (c) The phase space volume. The monotonically increasing solid line indicates the phase space volume of the part of the kinematical locus above the point where it contacts to a vertical line. The phase space volume of the part below the point are indicated by the broken line. The two peaked solid line indicates the projected energy spectrum at the 4.92 MeV resonance. The two peaked broken line indicates the spectrum divided by the phase space volume.

$$a_1=(m_1m_0E_0)^{1/2}/(m_0+m_t).$$

Analogous relation hold for E_{31} and E_{12} with

$$E_2{}^c=[(E_2)^{1/2}-a_2\cos\theta_2]^2+(a_2)^2\sin^2\theta_2,$$
$$a_2=(m_2m_0E_0)^{1/2}/(m_0+m_t),$$

and

$$E_3{}^c=E_{tot}{}^c-E_1{}^c-E_2{}^c.$$

The subscript t indicates the target particle. This is shown in Fig. 3(b).

The differential cross section for a spectrum projected on the E_1-axis is written in the form

$$\frac{d^3\sigma}{d\Omega_1 d\Omega_2 dE_1}=\frac{2\pi}{\hbar^2}\cdot\frac{\mu_0}{k_0}|M|^2\rho(E_1), \tag{5}$$

where $\mu_0=m_0m_t/(m_0+m_t)$ and $\hbar k_0$ is the absolute value of the relative momentum between the projectile and target. M is the matrix element of the reaction, and its form depends on the dynamics of the reaction. $\rho(E_1)$ is the phase space volume, and is given;

$$\rho(E_1)=\frac{h^{-6}m_1m_2m_3p_1p_2}{(m_2+m_3)+\dfrac{m_2(\boldsymbol{p}_1-\boldsymbol{p}_0)\cdot\boldsymbol{p}_2}{\boldsymbol{p}_2{}^2}}. \tag{6}$$

This is shown in Fig. 3(c).

2.2 Reation Dynamics

Two processes can be considered as the decay mechanism of $^{12}C^*$,

$$p+{}^{11}B\rightarrow{}^{12}C^*\rightarrow\alpha_1+{}^8Be^*\rightarrow\alpha_1+\alpha_{11}+\alpha_{12}, \tag{7}$$

and

$$\rightarrow\alpha+\alpha+\alpha. \tag{8}$$

(7) is the sequential decay, and (8) is the direct three α decay. In the case of (7), if the level width of the intermediate state $^8Be^*$ is fairly narrow, the first step is the two body decay and energy of α_1 that enters the detector 1 or 2 is definite. Furthermore as the decay of $^8Be^*$ is two body decay, the energy of α_{11} or α_{12} detected as a partner of α_1 is definite. So the two-dimensional energy spectrum of coincident α particles is expected to show sharp peaks on the locus and the projected energy spectrum of coincident particles will also show peaks at $E_1=E_{\alpha_1}$ and $E_1=E_{\alpha_{11}}$ (or $E_{\alpha_{12}}$). Then the relative energy between α_{11} and α_{12} is equal to the binding energy to form $^8Be^*$. Actually, as the level width of $^8Be^*$ is large, the peaks at $E_1=E_{\alpha_1}$ and $E_1=E_{\alpha_{11}}$ (or $E_{\alpha_{12}}$) are broad and the region, where the peaks overlap and are distorted, becomes large. Besides the spectrum may be distorted by the effect of α_1 on the decay of $^8Be^*$, for example, the final state interaction,[23] the effect of the Coulomb force and the rescattering phenomena.[24] The last phenomena may occur when α_{11} or α_{12} is emitted from $^8Be^*$ in the same direction as α_1 with sufficiently high energy. Furthermore, if the condition of detection is not suitable, the phase space volume remarkably distorts the spectrum.

In the case of (8), the direct three α decay, the relative energy of any pair of final three particles is, in principle, allowed to take any value smaller than the maximum value. If any pair of the particles do not interact in the final state and if the distribution does not depend on the angular momentum of the decaying state of ^{12}C, the spectrum must show the shape of the phase volume as is shown in Fig. 3(c). However, in general, when any pair of the particles stay in the interaction volume for sufficiently long period, they interact each other and the spectrum is naturally expected to show discrepancy in the region where the relative energy is smaller than a value.[21] If the distribution depends on the angular momentum of the decaying state, the situation may become very complicated as is described in the "generalized angular momentum

theory."[18]

Thus to decide the decay mechanism one should measure the coincidence energy spectrum under the detection condition at least including following ones.

i) The difference of the energies E_{α_1} and $E_{\alpha_{11}}$ (or $E_{\alpha_{12}}$) which are expected from the sequential decay mechanism is large enough to separate the peaks sufficiently.

ii) In the spectrum there is a region where all of three relative energies are simultaneously larger than a value which is to be determined experimentally.

iii) The phase volume does not extremely distort the shape of the spectrum.

These conditions are realized in this experiment. Fig. 4 is the velocity diagram which shows the kinematical relation in the experiment with the tandem Van de Graaff accelerator. $\vec{OA}$ is the velocity of the center of mass or the compound nucleus $^{12}C^*$. In the sequential decay, α_1 produced in the first step flies in an arbitrary direction with the velocity represented by the radius of the large cricle $\overset{\frown}{BFH}$ around A in the center of mass system. The accompanying $^8Be^*$ (1st) flies in the opposite direction to that of α_1 with the velocity represented by the radius of the length of $\overline{AC}$. Since the level width of $^8Be^*$ (1st) is as large as 1.5 MeV, length of $\overline{AB}$ and $\overline{AC}$ vary withe the excitation energy E_x of $^8Be^*$ as is shown in Fig. 4. In the second step, ^8Be (1st) decays into α_{11} and α_{12}. Their directions of fligh are arbitrary but opposite to each other in the center-of-mass system of $^8Be^*$. When α_1 enters the detector 1 (denoted D1) in the direction $\vec{OB}$ and $^8Be^*$ (1st) flies in the direction $\vec{AC}$ in the center of mass system, then the velocities of α_{11} and α_{12} are given by

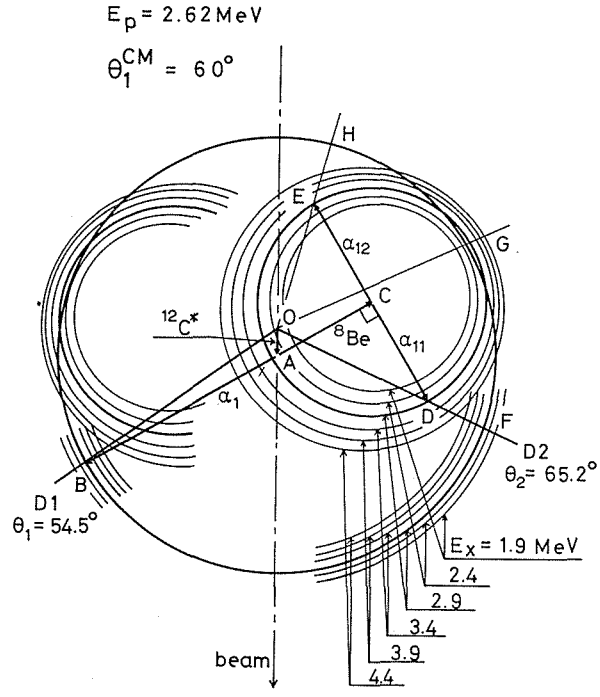

Fig. 4. The velocity diagram of the reaction $^{11}B+p\rightarrow{}^{12}C^*\rightarrow\alpha_1+{}^8Be^*(2^+)\rightarrow\alpha_1+\alpha_{11}+\alpha_{12}$.

radii of the small circles around C. The magnitude of the velocity varies corresponding to E_x as is shown in Fig. 4. If the detector 2 (denoted D2) is set in the direction of $\vec{OF}$, it detects α_{11} which has the velocity represented by $\vec{OD}$ in coincidence with α_1.

In this arrangement of the detectors, of course, D2 detects α_1 with the velocity $\vec{OF}$ in coincidence with the accompanying α_{11} (or α_{12}), which is detected in D1. Therefore, in D2 enter two kinds of α particles with different velocities $\vec{OD}$ and $\vec{OF}$. In this case, as velocities $\vec{OD}$ and $\vec{OF}$ are sufficiently different from each other, energies of α_1 and α_{11} detected in D2 are enough different to separate their peaks sufficiently. However, if D2 is set in the direction of $\vec{OG}$, velocities or energies of α_1 and α_{11} detected in D2 are not sufficiently different. The peaks of α_1 and α_{11} overlap each other. As to α particles detected in D1, the situation is almost same because the velocity of the center of mass is small compared with those of outgoing α particles. Thus, when D1 is set in the direction of $\vec{OB}$, it is better to set D2 in the direction of $\vec{OF}$ than to set in the direction of $\vec{OG}$ with respect to condition i). In this point, it is as good to set D2 in the direction of $\vec{OH}$ as in the direction of $\vec{OF}$. But, it is worse with respect to the condition iii) to set D2 in the direction of $\vec{OH}$, because the phase space volume becomes extremely large as a part of E_x in the tail of ^{8}Be* (1st) and becomes zero below the part.

In practice, the direction $\vec{OF}$ is so determined that the velocity of α_{11} in the center-of-mass system of ^{8}Be* make a right angle with that of ^{8}Be* (1st) in the center-of-mass system. When the direction of D1 is changed, the direction of D2 is also changed so as to remain the angular relation mentioned above. In this arrangement of D1 and D2, the condition ii), as well as the condition iii), is satisfied as is shown in Fig. 13, 14 and 15. Moreover, these detector arrangements have a merit that a nearly correct spectrum of α_1 is expected to be measured in D1. Although the angle, between the velocity of α_{11} in the center-of-mass system of ^{8}Be* and that of ^{8}Be* (1st) in the center-of-mass system, varies in the region of about $90°\pm10°$ corresponding to the level width of ^{8}Be*, the angular distribution of the $\alpha-\alpha$ scattering is almost flat in that region.

Thus these arrangements of D1 and D2 are chosen throughout the coincidence measurements with the tandem Van de Graaff accelerator. In the coincidence measurements with the Cockcroft-Walton accelerator, slightly different arrangements are chosen but they satisfy the conditions i), ii) and iii).

3. Experimental Procedure

3.1 Experiment with the Cpckcroft-Walton accelerator

The proton beam is accelerated with the Cockcroft-Walton accelerator in the Department of Physcis, Kyoto Univ. The beam is analyzed with a 90° magnet, and defined by two slits. One is of 2.5 mm radius and placed at the exit of the analyzer, the other is of 1.5 mm radius and placed at the entrance of the scattering chamber. The slits are separated by 1.5 m. The beam intensity is a few μA throughout the experiment. The target is a self-supported thin foil of natural Boron (81.2 % ^{11}B+18.8 % ^{10}B) with thickness of 19 μg/cm^2. This corresponds to the energy loss of about 12 keV for 200 keV proton. The

target is set at such an angle that both of the energy losses of α particles entering the detectors are as small as possible. Those energy losses are smaller than several ten keV and may be neglected. The detectors used are two 500 μ surface barrier solid state detectors. They are set on a pair of turning tables which can be independently moved around a common axis. They are moved on the reaction plane that include the beam axis and the target. The solid angle of each detector is defined by a slit in front of it, and they are both 6.0×10^{-3} steradians. Fig. 5 shows the electronic circuit system used. Resolving times of fast coincidence systems are both about 80 nsec in 2τ. Levels of all the fast discrininators are so set to cut off the background as possible and pulses from α particles of energy less than about 2 MeV are cut off. The overall energy resolution of the electronic circuit system is about 250 keV for 5.5 MeV α particles. The Nuclear Data 1024 ch. pulse height analyzer is used in two dimensional mode (64 ch $\times$ 16 ch).

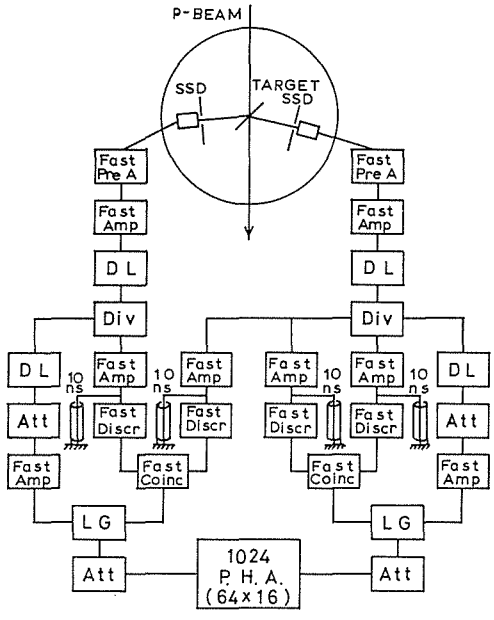

Fig. 5. The block diagram of the electronic circuit system used in the experiment with the Cockcroft-Walton accelerator.

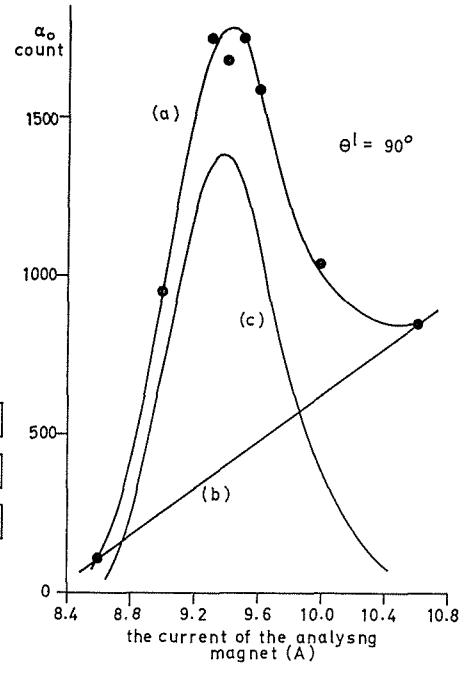

Fig. 6. The excitation function of the differential cross section of α_0. The 163 keV resonance (c) was obtained by substracting the tail part (b) of the upper resonance from the excitation function (a).

In the experiment with the Cockcroft-Walton accelerator, at the first step, the excitation function of α_0 is measured for the calibration of the incident proton energy with respect to the current of the magnetic analyzer. The result is shown in Fig. 6. The 163 keV resonance correspond to 9.4 A of the current of the magnetic analyzer.

Coincidence measurements are carried out under the following conditions;

a) $\theta_1=\theta_2=60°$, $E_p=138$ keV, 152 keV, 163 keV, 175 keV, 188 keV, 215 keV, 232 keV,

b) $E_p=163$ keV, $\theta_1=60°$ and $\theta_2=60°$, 70°, 90°,

c) $E_p=215$ keV, $\theta_1=60°$ and $\theta_2=60°$, 70°, 90°.

The primary coincidence specta are measured as two dimensional in the (64 ch $\times$16 ch) configuration. Pulses from the detector at θ_1 are led into the 64 ch. side and those from the detector at θ_2 are led into the 16 ch. side. The integrated beam current is 9000 μCoulomb for every run. The final, single dimensional spectra are obtained from the primary data by projecting the yields for each channel of the 64 ch. axis on the kinematical locus. By means of this method, the energy resolution of the projected energy spectra are improved.

3.2 Experiment with the tandem Van de Graaff accelerator

The proton beam is accelerated with the tandem Van de Graaff accelerator in the Department of Physics, Kyoto Univ.[25] The beam is analyzed by a 90° magnet and stabilized by the slit stabilizer system. The energy spread of the beam is about 0.1 % of the beam energy. The beam is guided into the scattering chamber through a switching magnet and a collimater system of triple slits. The beam spot on the target is 3 mm in diameter. The target used are self-supporting thin foils of eneriched ^{11}B prepared with the vacuum evaporation method using an electron bombarding unit. Two targets are used. One is of 65 μg/cm^2 thick and is used for measurements of single α spectra and energy scales. The other is of 230 μg/cm^2 thick and is used for measurements of coincidence energy spectra. The target thickness is determined from the energy loss for 5.476 MeV Am^{241}-α particles. Throughout the coincidence measurement the target is set at an angle of 45° with respect to the beam axis, with energy losses of α particles entering the detector 1 being smaller. The energy loss of the incident proton in the target is a few ten keV.

The detectors used are two 100 μ surface barface solid state detectors. One is mounted on the turning table and the other on the turning arm, which can be moved independently around the common axis. In front of the detector 1 is set a rectangular slit of 8 mm high and 3 mm wide, and in front of the detector 2 is set a circular slit of 8 mm in diameter. The solid angles are 2.90 $\times10^{-3}$ steradians and 6.25$\times10^{-3}$ steradians, respectively. An RCA Victor $p-n$ junction solid state detector is used as the beam monitor, which is set at an angle of 155° to the direction of the incident beam. With it, elastically scattered protons are counted.

The block diagram of the electronic circuits used is shown in Fig. 7. Because the protons scattered elastically give rise a large count of accidental coincidences, the spectrum of accidental coincidences has to be measured simultaneously with the coincidence spectrum. Each pulse from the preamplifires is divided into the energy pulse and the timing pulse. The energy pulse is immediately led into the pulse height analyzer. The timing pulse is divided into two pulses after being amplified and discriminated.

The level of discrimination is set so as to cut off the background and to count pulses higher than those from α particles of about 1 MeV. The devided pulses are again pulseshaped and led into two fast coincidence circuits. One is used for the coincidence gate signal and the other is for the gate signal of

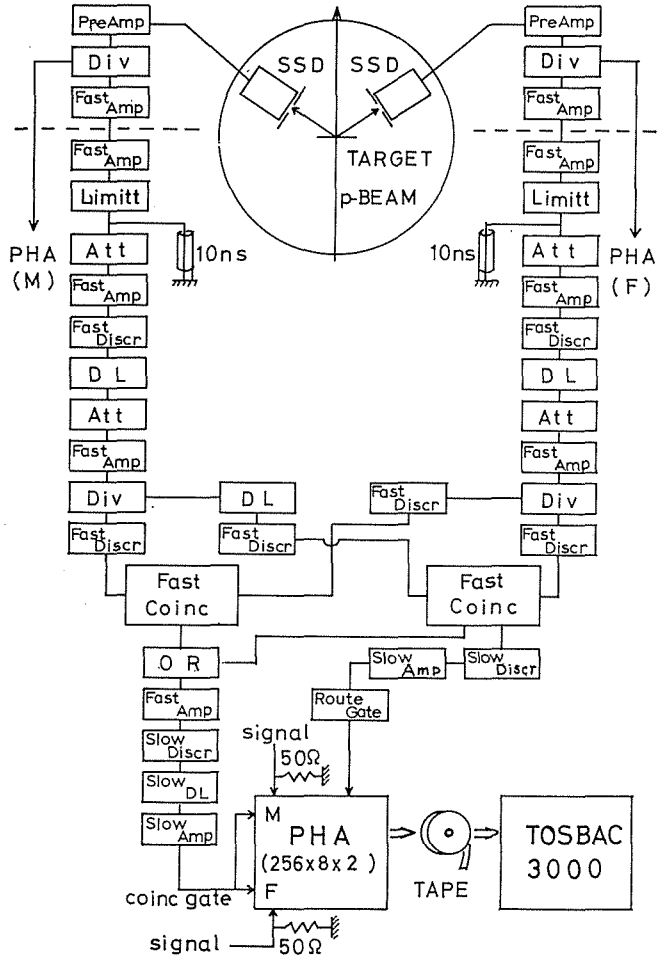

Fig. 7. The block diagram of the electronic circuit system used in the experiment with the tandem Van de Graaff accelerator.

the accidential coincidence. One of the input pulses led into the coincidence circuit is delayed by 100 nsec in the case of the accidental coincidence. The resolving times of both the coincidence systems are 45 nsec in 2τ. Output pulses of them are mixed and converted into slow pulses and then led into the pulse height analyser as the coincidence gate signals. Nuclear Data 4096 ch. pulse height analyzer is used in the (256 ch × 8 ch × 2) configuration. In one of (256 ch × 8 ch), the coincidence spectrum is measured and in the other the accidental coincidence spectrum is simultaneously measured by means of the route gate. Pulses from the detector 1 are analyzed in the 256 ch side and those from the detector 2 in the 8 ch side. In this method, the width of the obtained peak is about 130 keV in the full width of half maximum for coincident α particles of about 8MeV which are produced in the reaction ($^{11}B+p\rightarrow\alpha_0+{}^{8}Be\rightarrow\alpha_0+\alpha_{01}+\alpha_{02}$) with the thin target. On the main part of the kinematical locus, yields of the accidental coincidence are less than five percents. However, on the part where elastically scattered protons overlap, counts of accidental coincidences increase.

The data are printed out with the OPTIKON unit and punched out on paper tapes. Then they are processed with the electronic computer TOSBAC-3000. The spectra of true coincidence are obtained by subtracting accident coincidence yields from coincidence yields. As the final state of data, projected energy spectra of coincident α particles are obtained from the true coincidence spectra by projecting the yields on the kinematical locus onto the 256 ch axis.

The energy scales are decided by detecting α_0 and α_{01} (or α_{02}) in coincidence.

Coincidence measurements are carried out under the following conditions;

a) $\theta_1^{CM}=90°$, at eleven energies of E_p between 2.00 MeV and 4.00 MeV,

$\theta_1^{CM}=60°$, at nineteen energies between 2.20 MeV and 4.00 MeV,

b) $\theta_1^{CM}=90°$, at eight energies between 4.80 MeV and 5.30 MeV,

c) $\theta_1^{CM}=30°$, 40°, 50°, 60°, 70°, 80°, 90°, 100° and 110°, at $E_p=2.62$ MeV and 4.92 MeV,

where θ_1^{CM} indicates the angle of the detector 1 in the center of mass system. The angle of the detector 2 is set as described in the section 2.2. Measurements under conditions a) and b) are intended to investigate the energy dependence of the shape of the spectrum. Measurements under the condition c) is intended to examine whether the characteristics of the spectra at the resonances vary with the angular condition.

4. Experimental Results

4.1 Experimental Results at $E_p=138$ keV$\sim$232 keV

The shapes of projected energy spectra of coincident α particles at $\theta_1=\theta_2=60°$ strongly depend on the incident proton energy (Fig. 8).

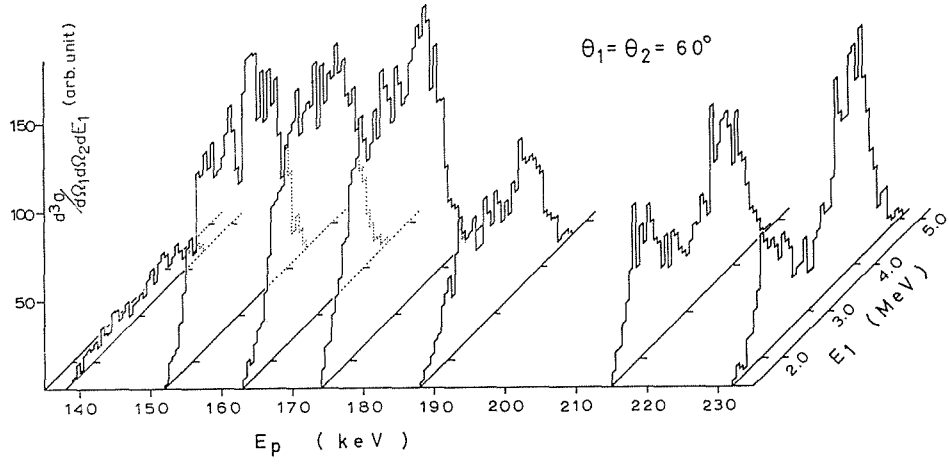

Fig. 8. The dependence of projected energy spectra on the incident energy.

At the 163 keV resonance, spectra show a broad peak with a flot top. The flat part extends from $E_1\cong 2.3$ MeV (where $E_{31}\cong 3.0$ MeV) to $E_1\cong 3.9$ MeV (where $E_{23}\cong 3.2$ MeV). The shape of the flat part well agrees with that of the phase space

volume. As the energy of the incident proton becomes higher, two peaks come out. At the top of the higher E_1 peak, E_1 is nearly equal to 3.9 MeV, which corresponds to E_{23} of about 3.2 MeV. The width of the peak is about 1 MeV, which corresponds to about 1.4 MeV in E_{23}. At the top of the lower E_1 peak, E_1 is nearly equal to 2.2 MeV, which corresponds to E_{31} of about 3.0 MeV. The width of the peak is nearly equal to 1 MeV, which corresponds to 1.3 MeV in E_{31}. With respect to the relative energies and the widths, the higher peak well agrees to the α_1 peak and the lower peak to the α_{11} peak expected from the sequential decay mechanism.

It is very interesting that the lower slope of the borad peak at the resonance begins to fall at higher energy than that of the lower peak at $E_p=215$ keV, and that the higher slope of the broad peak begins to fall at lower energy than that of the higher peak. Because the discriminators probably cut off those parts with E_1 or E_2 below 1.8 MeV, the differences may be larger than appears in Fig. 8.

In Fig. 9 are shown angular correlations at the resonance and off the resonance between $\theta_1=60°$ and $\theta_2=60°$, 70°, 90°. Because of the poor statistics, it is not clear if α_1 and α_{11} peaks separate at $E_p=215$ keV, $\theta_1=60°$ and $\theta_2=70°$. At $E_p=215$ keV the yield is appreciably enhanced where the kinematical loci of α_1 and α_{11} intersect with each other ($\theta_1=60°$ and $\theta_2=90°$), but such an enhance-

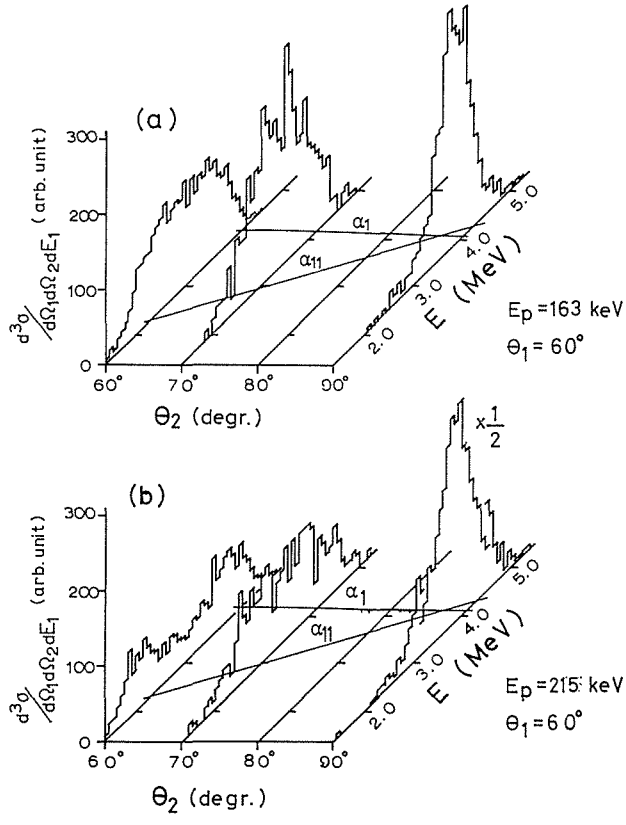

Fig. 9. Angular dependences of projected energy spectra.

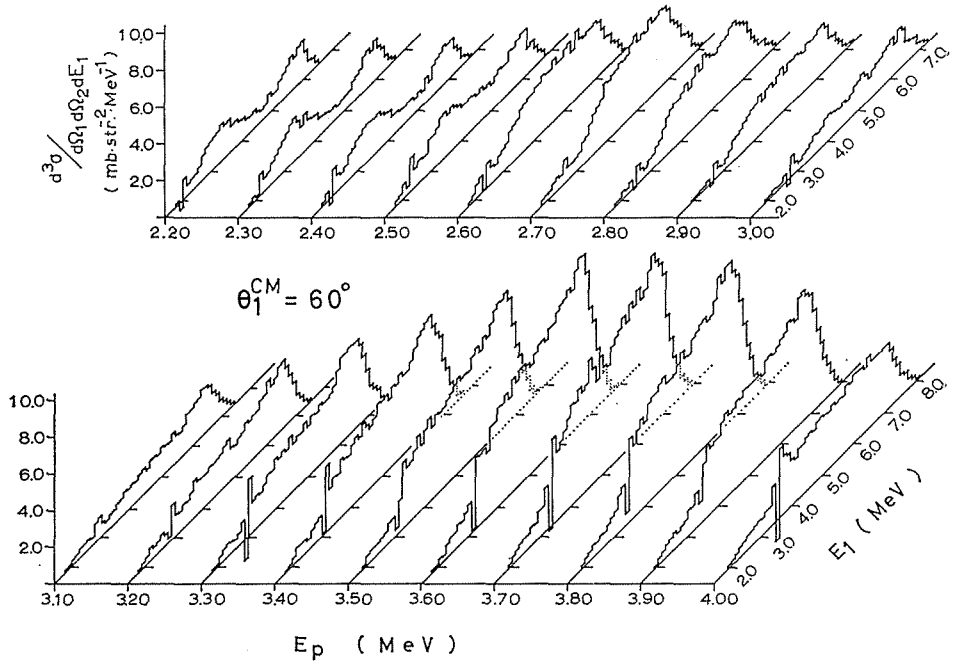

(a)

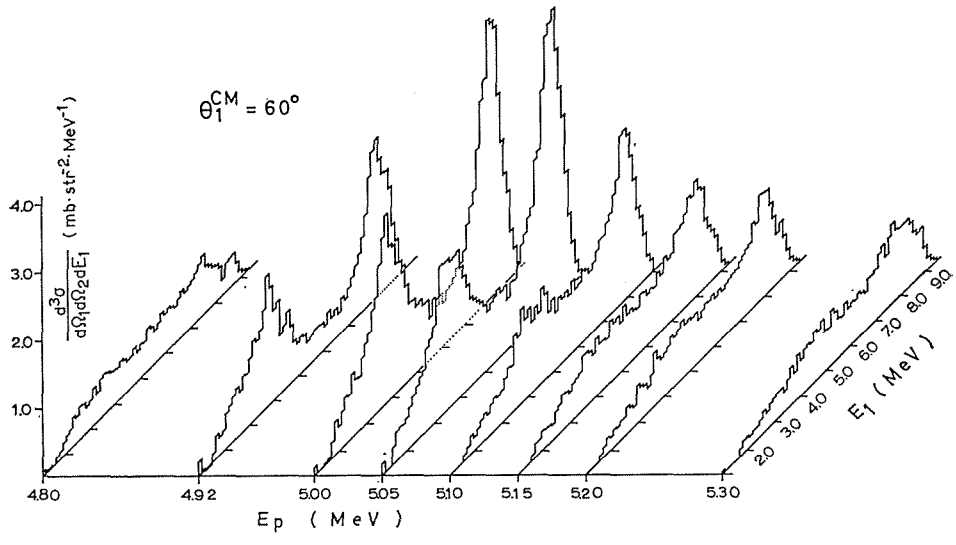

(b)

Fig. 10. The dependence of project energy spectra on the incident energy at the angular condition $\theta_1{}^{CM}=60°$.
(a) 2.20 MeV$\leqq E_p \leqq$4.00 MeV.
(b) 4.80 MeV$\leqq E_p \leqq$5.30 MeV.

ment is not seen at the 163 keV resonce.

4.2 Experimental Results at E_p=2.0 MeV~5.3 MeV

Energy dependences of projected energy spectra of coincident α particles are shown in Fig. 10 for $\theta_1^{CM}=60°$ and in Fig. 11 for $\theta_1^{CM}=90°$. They show strong dependence of the shape on the incident proton energy. Moreover, spectra seem to change their shapes corresponding to the resonances in the (p, α) channel as the vicinity of the 163 keV resonance. In this region, there are resonces at E_p=2.62, 3.5, 3.7, 4.92 and 5.11 MeV.[8] The shape of the spectrum varies clearly near these resonances.

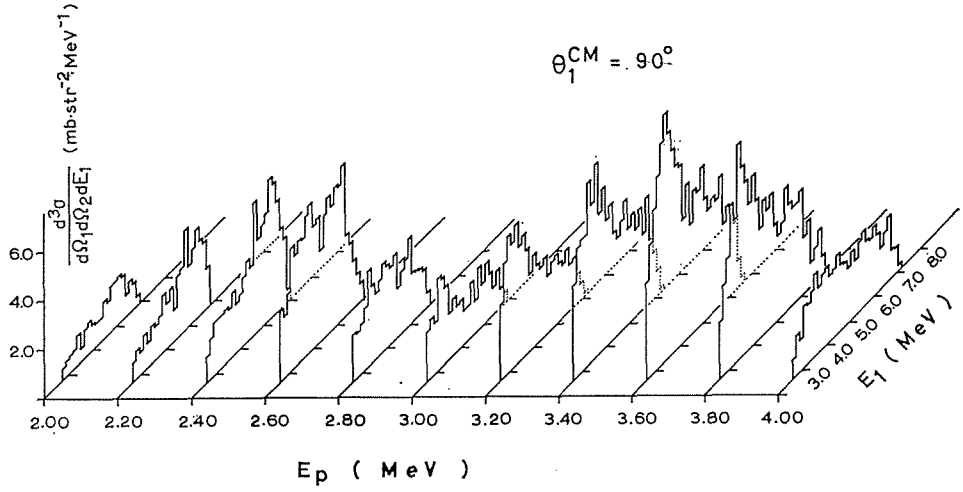

(a)

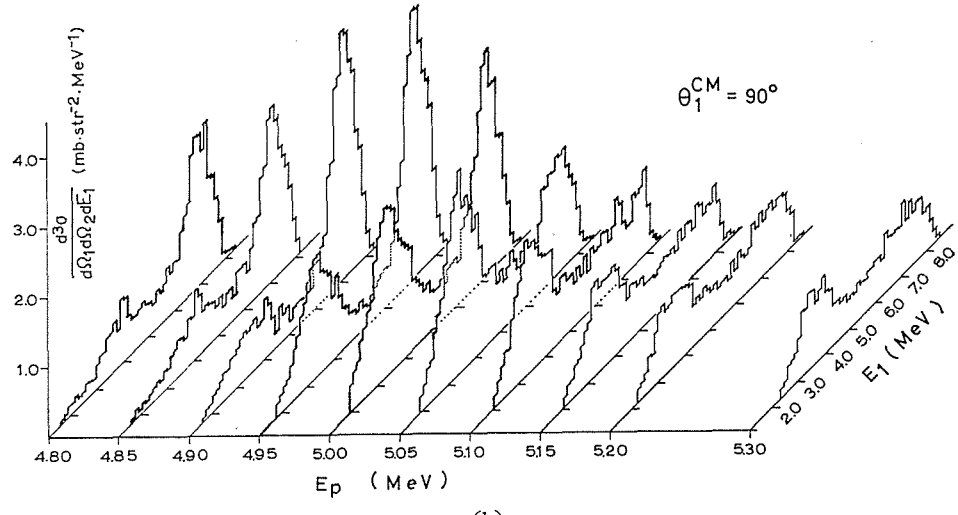

(b)

Fig. 11. The dependence of projected energy spectra on the incident energy at the angular condition $\theta_1^{CM}=90°$.
(a) 2.00 MeV$\leqq E_p \leqq$4.00 MeV.
(b) 4.80 MeV$\leqq E_p \leqq$5.30 MeV.

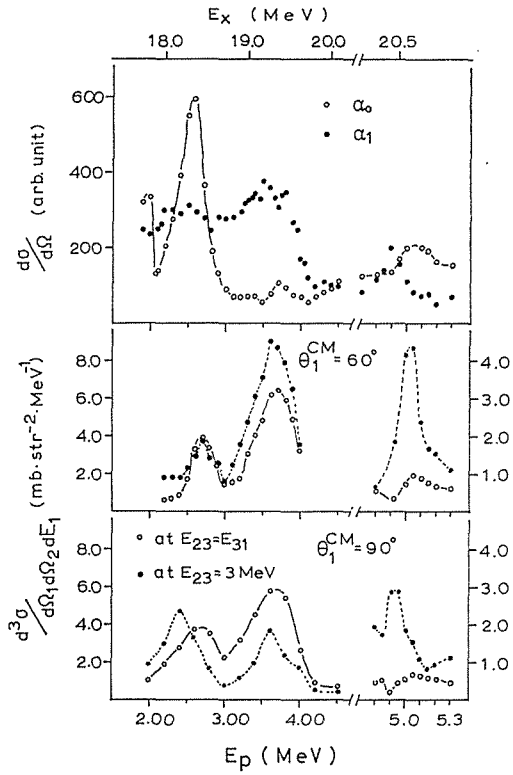

Fig. 12. Dependences of the differertial cross section upon the incident energy. The uppermost graph is the excitation function of the differential cross section of the reactions $^{11}B(p, \alpha_0)^8Be$ and $^{11}B(p, \alpha_1)^8Be^*$ (1st) at $\theta^{CM}=90°$. The middle is the excitation function of the differential cross section $d^3\sigma/d\Omega_1 d\Omega_2 dE_1$ at $\theta_1^{CM}=60°$, and the bottom is that at $\theta_1^{CM}=90°$. For both ○ indicates the differential cross section at $E_{23}=E_{31}$ and ● that at $E_{23}=3$ MeV.

Near the 2.62 MeV resonance, spectra show a broad peak with a flat top. The shape of the flat part well agrees to that of the phase space volume. These features well resemble those at the 163 keV resonance.

In the vicinity of $E_p=3.6$ MeV, spectra show complex shapes. They do not show two separated peaks, but show a broad peak rather like those of the 2.62 MeV resonance. However, there is a difference. The flat tops of the latter well agree with the shapes of the phase volume for both $\theta_1^{CM}=60°$ and $\theta_1^{CM}=90°$. On the other hand, the former has a small bump at the high E_1 side for $\theta_1^{CM}=60°$ and at the low E_1 side for $\theta_1^{CM}=90°$. This is probably due to the fact that in this region of the incident energy two broad resonances centered at $E_p=3.5$ MeV and $E_p=3.7$ MeV overlap closely.

Near the 4.92 MeV resonance, spectra at $\theta_1^{CM}=60°$ show two peaks at $E_1=8.1$ MeV (where $E_{23}=2.7$ MeV) and at $E_1=3.6$ MeV (where $E_{31}=2.7$ MeV), spectra at $\theta_1^{CM}=90°$ also show two peaks at $E_1=7.1$ MeV (where $E_{23}=2.7$ MeV) and at $E_1=3.2$ MeV (where $E_{31}=2.8$ MeV). The widths of the higher E_1 peaks are 1.1 MeV for $\theta_1^{CM}=60°$ and 1.0 MeV for $\theta_1^{CM}=90°$, both of which correspond to 1.6

MeV in E_{23}. These well agree with the α_1 and α_{11} peaks expected from the sequential decay mechanism.

Near the 5.1 MeV resonance, the tail of the 4.92 MeV resonance makes two peaks. Heights of these peaks gradually diminish with the higher incident energy. However, both of the excitation functions of the yields at $E_1 \cong 6$ MeV and $\theta_1^{CM}=60°$ and at $E_1 \cong 5$ MeV and $\theta_1^{CM}=90°$ make peaks having maximum value at $E_p=5.1$ MeV.

In Fig. 12 are shown excitation functions of the differential cross sections at $E_{23}=3$ MeV which corresponds to the top of the α_1 peak and at $E_{23}=E_{31}$ which corresponds to the flat part. The middle of Fig. 12 is the excitation function of the coincident α particles at $\theta_1^{CM}=60°$ and the bottom is that at $\theta_1^{CM}=90°$. The uppermost is excitation functions of differential cross section for α_0 and α_1 measured without the cincidence method.

Excitation functions at $E_{23}=E_{31}$ show peaks at about 2.6 MeV, at about 3.7 MeV and at about 5.1 MeV. Excitation function at $E_{23}=3$ MeV and $\theta_1^{CM}=60°$ shows peaks at about 2.6 MeV, at about 3.6 MeV and at about 5.0 MeV. That at $E_{23}=3$ MeV and $\theta_1^{CM}=90°$ shows peaks at about 2.4 MeV, at about 3.6 MeV and at about 4.9 MeV. The peak at about 2.4 MeV seems to be a new resonance, because spectra at $E_p \cong 2.4$ MeV show two peaks and clearly different features from spectra at the 2.62 MeV resonance. But it is not so clear, because the excitation function at $E_{23} \cong 3$ MeV and $\theta_1^{CM}=60°$ shows a peak at $E_p=2.6$ MeV. These peaks can be also interpreted to be formed by overlapping of tail parts of the 2.62 MeV resonance and resonances lower than 2 MeV.

The excitation function at $E_{23}=E_{31}$ does not change the position of the peak at about 5.1 MeV either at $\theta_1^{CM}=60°$ or at $\theta_1^{CM}=90°$. On the other hand the excitation function at $E_{23}=3$ MeV changes the position of the peak near the 4.92 MeV resonance at $\theta_1^{CM}=60°$ and at $\theta_1^{CM}=90°$. This means that the flat part does not come from the same source that makes the tail part of the 4.92 MeV resonance. Rather the flat part is considered to come from the same sort of the broad peak of the 2.62 MeV resonance.

In Fig. 13 and Fig. 14, angular dependence of the spectra are shown for the 2.62 MeV resonance and for the 4.92 MeV resonance, a) corresponds to $\theta_1^{CM}=30°$, b) to $\theta_1^{CM}=40°$, c) to $\theta_1^{CM}=50°$, d) to $\theta_1^{CM}=60°$, e) to $\theta_1^{CM}=70°$, f) to $\theta_1^{CM}=80°$, g) to $\theta_1^{CM}=90°$, h) to $\theta_1^{CM}=100°$ and i) to $\theta_1^{CM}=110°$. In these figures, the ordinate is the differential cross section divided by the phase spase volume, which is proportional to $|M|^2$ in the eq. (5). E_{23}, E_{31} and E_{12} mean the relative energies.

For the 2.62 MeV resonance, all spectra divided by the phase space volume clearly show flat tops. These values fall down from where the relative energy E_{23} or E_{31} becomes less than about 3 MeV. This value slightly varies with the condition.

For the 4.92 MeV resonance all spectra show two peaks. Peak at the higher energy are centered at a same point where E_{23} is about 2.7 MeV. Full width of the half maximum of those peaks is about 1.6 MeV in E_{23}. These well agree to the binding energy for two α particles to form the first excited state of ^8Be and to the width of the level. Full width of the half maximum of lower broad peaks is also about the same. These confirm that those peaks correspond to α_1 and α_{11} (or α_{12}) peaks, and that the decay mechanism is sequential. The variation of height of the peaks reflects the angular distribution of α_1.

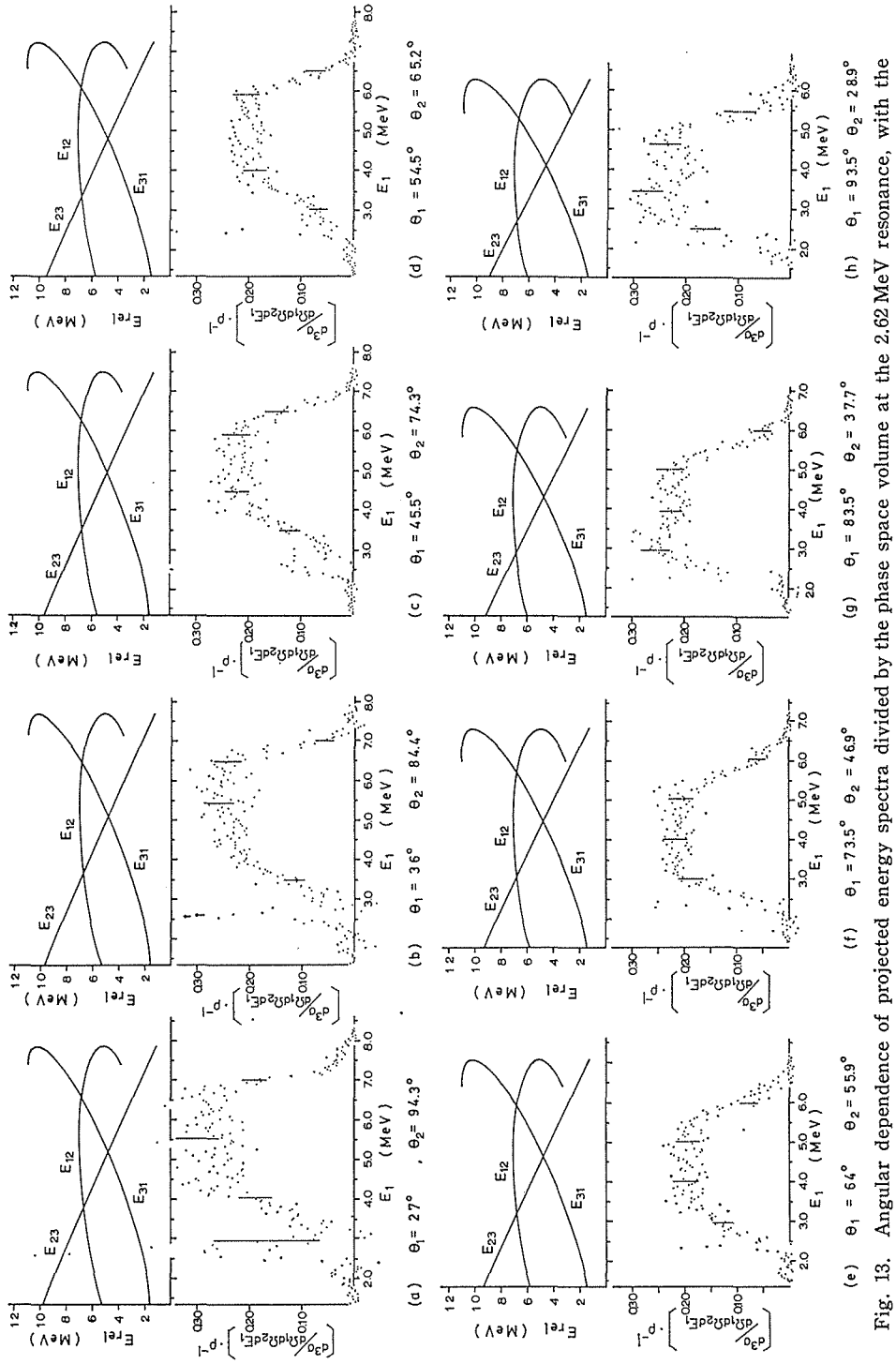

Fig. 13. Angular dependence of projected energy spectra divided by the phase space volume at the 2.62 MeV resonance, with the relative energies. The dimension of the $(d^3\sigma/d\Omega_1 d\Omega_2 dE_1)\cdot\rho^{-1}$ is $[mb\cdot(a.m.u.)^{-3}\cdot(str)^{-2}\cdot(MeV)^{-2}]$.

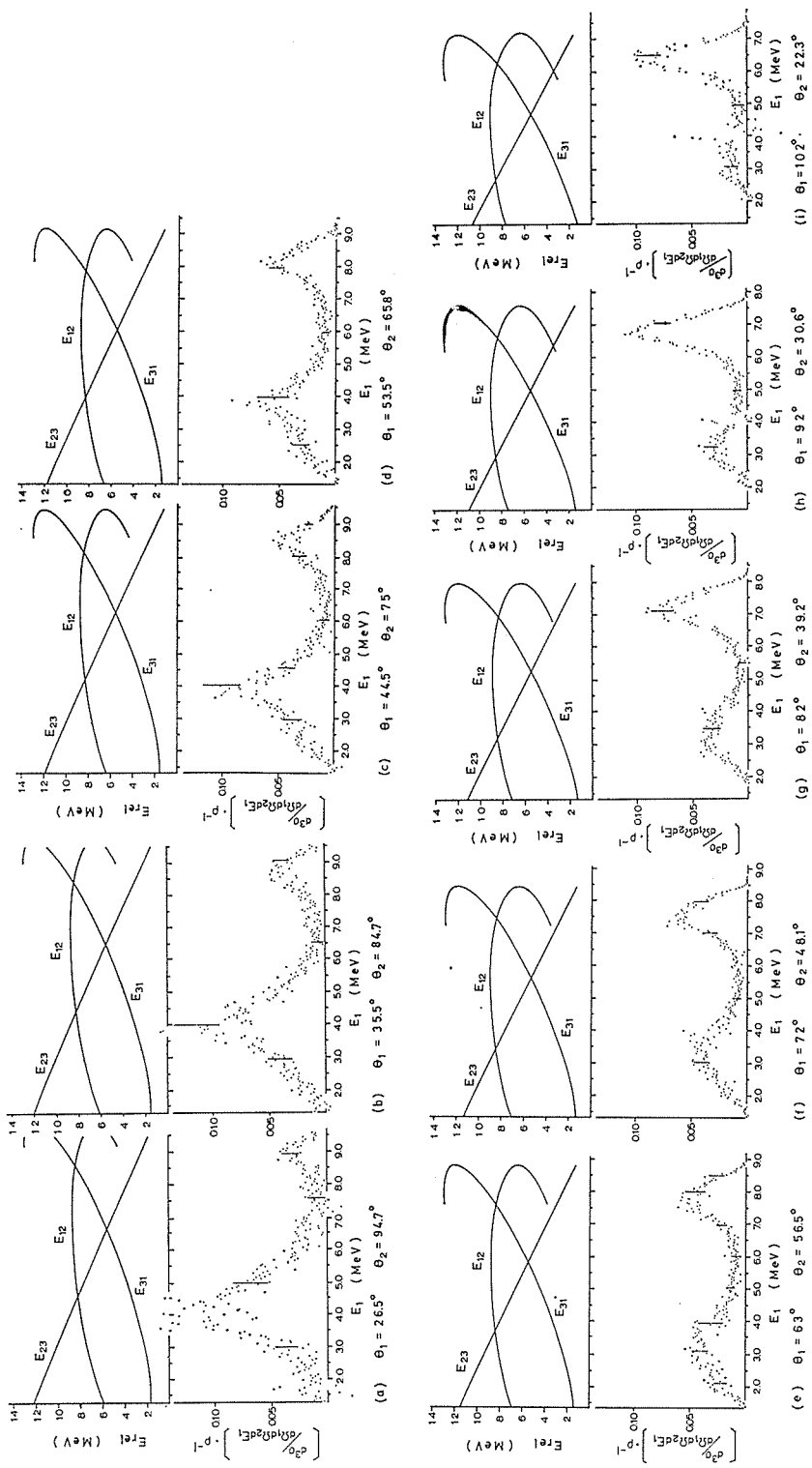

Fig. 14. Angular dependence of projected energy spectra divided by the phase space volume at the 4.92 MeV resonance, with the relative energies.

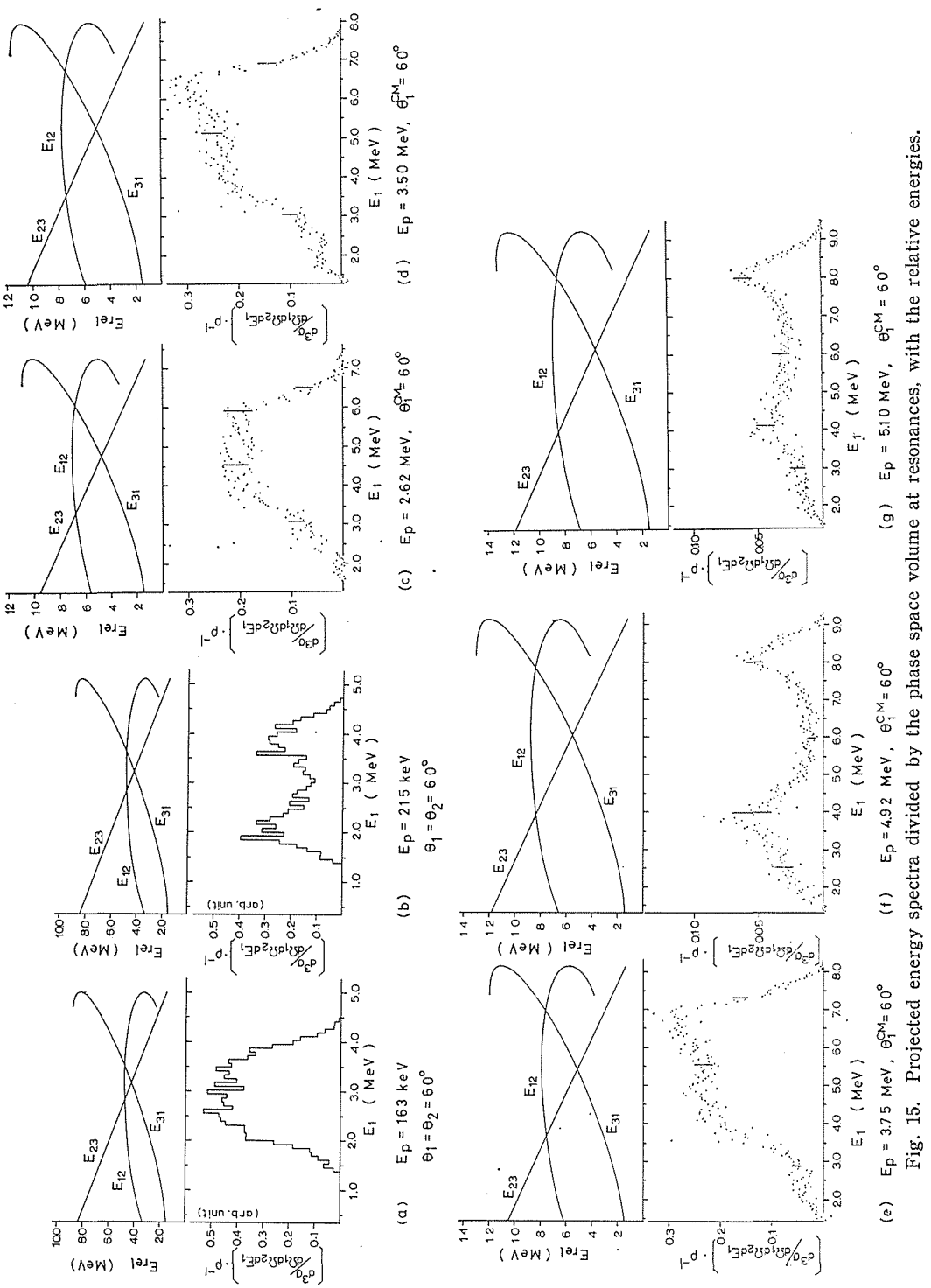

Fig. 15. Projected energy spectra divided by the phase space volume at resonances, with the relative energies.

To make clear the dependence of the shape of the spectrum upon the resonance, spectra divided by the phase space volume at $E_p=165$ keV, 215 keV, 2.62 MeV, 3.5 MeV, 3.75 MeV, 4.92 MeV and 5.1 MeV are shown in Fig. 15.

It is very interesting that the spectra at $E_p=3.5$ MeV and 3.75 MeV show such a shape that is expected from superposition of following two types of spectra with some ratio. One is the type of spectra at the 2.62 MeV resonance, and the other is the type of spectra at the 4.92 MeV resonance. This is suggested in following points. The general feature of the spectral shape resembles rather that of the 2.62 MeV resonance. In the part corresponding to the flat top, there appear one or two bumps which show some angular dependence. The upper and lower slopes show two fold structures. In this energy region, there are two broad resonances contered at 3.5 MeV (1^-; T=1) and at 3.75 MeV (2^+; T=0). Thus, it may be considered that one of them makes the part which resembles spectra at the 2.62 MeV resonance and the other the part which resembles spectra at the 4.92 MeV resonance.

In summary, following results are obtained.

i) In our condition of detection, energy spectra of coincident α particles clearly show dependence on the resonances.

ii) At the 4.92 MeV resonance, at about 215 keV and at about 2.4 MeV, spectra show well separated two peaks which have the energies and the widths expected from the sequential decay mechanism.

iii) At the 2.62 MeV resonance, as the 163 keV resonance, spectra show only one broad peak with a flat top which well agrees with the phase space volume. Spectra also show relatively sharp falling down at the energies where one of the relative energies becomes lower than about 3 MeV.

iv) At about 3.6 MeV and at the 5.1 MeV resonance, spectra show complex shapes which may be considered as superposition of two types of spectra.

5. Discussion

In this section the results are discussed on the decay mechanism and on the structures of higher excited states of ^{12}C.

i) Spectra at the 163 keV resonance and at the 2.62 MeV resonance

In the present work, at the 2.62 MeV resonance almost same specta are obtained as at the 163 keV resonance, that show only one broad peak with a flat top. At the 163 keV resonance, D. Dehnhard et al.[11] reported the same shape of spectra and concluded the direct three α dechanism. On the contrary, Y. S. Chen et al. concluded the sequential decay mechanism from their experimental results. At $E_p=2.65$ MeV, J. D. Bronson et al.[13] concluded the sequential decay mechanism with the interference effects.

The detection condition selected in the present work is that the α_1 and α_{11} peaks expected from the sequential decay mechanism can be separated as distant as possible. In this condition the overlap of the α_1 and α_{11} peaks is fairly diminished, so the interference effects may be suppressed. In fact at the 4.92 MeV resonance, at about 2.4 MeV and at about 215 keV, spectra show clearly two separated peaks which are expected from the sequential decay mechanism. Nevertheless, spectra at the 163 keV resonance and at the 2.62 MeV resonance show widely different features from those of the sequential decay.

Natural explanation of these spectra can be obtained by taking account into the more significant characteristics of the detection condition in the present work. That is, there is a sufficiently wide region in which all the three relative energies of the final α particles are simultaneously higher than about 3 MeV. This is the essential point of this work different from the works of J. D. Bronson et al. and others. Following three points should be mentioned with resport to this.

a) In general, for the direct three body decay the energy spectrum of a particle shows the shape of the phase space volume. However, when the observed particle has near maximum energy and the other two particles have nearly zero relative energy, the two particles must suffer some interactions, and their emission is suppressed. Consequently the direct three body decay is suppressed.[21] This effect is expected whenever a pair of particles have low relative energy. From these effects the energy spectrum for the direct three body decay is expected to show the shape of the phase space volume where relative energies of all the pairs are sufficiently high and to show deviation from it where relative energy of any pair becomes lower than a critical value.

b) In the previously published papers on the decay mechanism at these resonances, authors were mainly interested in those spectra measured where energies of α_1 and α_{11} approach to each other.[11,13~16] On this condition, relative energies E_{23} and E_{31} are always lower than about 3 MeV, or if they become higher, the region is very narrow. The spectra show one or two separated peaks, but they are so distorted not to be expected from the simple sequential decay mechanism. To explain them with the sequential decay mechanism some interference effects had to be introduced.

c) The spectra at these resonances obtained in the present experiment clearly show that shapes of them well agree to those of the phase space volume where all the relative energies are higher than about 3 MeV, and that they quickly fall down where E_{23} or E_{31} becomes lower than about 3 MeV.

From these it seems natural to consider that there is the critical value at about 3 MeV. Then, the decay mechanism is considered to be the direct three body decay. Below the critical value, the final state interaction affects the α particles to form the distorted peaks near E_{α_1} and $E_{\alpha_{11}}$. Thus, if one takes such a condition that has not a sufficiently wide region with all the relative energies higher than about 3 MeV, one can not clearly distinguish between the direct three α decay and the sequential α decay.

When two α particles separate from each other with the relative energy of 3 MeV, it takes about 3×10^{-22} sec. for them to reach the relative distance of 5 fm, which corresponds to the radius of interaction region. Therefore, when the excited state of ^{12}C decays directly to three α particles, if any pair of them have a relative energy higher than about 3 MeV, they separate so quickly that the effect of the final state interaction will be small. But if they have a relative energy lower than the value, the effect of the final state interaction will not be small or becomes important.

Consequently, at these resonances the decay mechanism can be considered as the direct three α decay.

ii) Spectra at the 4.92 MeV resonance, at about 215 keV and at about 2.4 MeV

The spectra at these energies do not show any enhancement in the region where all the relative energies becomes higher than about 3 MeV. These spectra show that the relative energy E_{23} at the top of the higher E_1 peak is neerly to that of the first excited state of ^8Be, and that the width of the peak is nearly equal to that of the first excited state of ^8Be. At the lower broad peak, the relative energy E_{31} and the width are also nearly equal to the first excited state of ^8Be. Shapes of the spectra at about 215 keV well agree with those at the 675 keV resonance observed by D. Kamke et al.[12] Therefore the former is considered to correspond to the tail part of the latter.

At about 2.4 MeV, specta clearly show the shape expected from the sequential decay mechanism. So they are not considered to come from the tail part of the 2.62 MeV resonance. The excitation function of the differential cross section at $E_{23}=3$ MeV and $\theta_1^{CM}=90°$ makes a peak in this vicinity, which suggests that there is a new resonance. The excitation function at $\theta_1^{CM}=60°$ shows such a peak at $E_p=2.6$ MeV. However, at $\theta_1^{CM}=60°$ the flat part which comes from the tail part of the 2.62 MeV resonance extends to the point where $E_{23}=3$ MeV, and the contribution from the part cannot be separated. To clear whether there is a new resonance or not, excitation functions at other angles should be measured. It is clear that in this method more detailed information is obtained than the method in which only one of three outgoing α particles is detected.

iii) Spectra at about 3.6 MeV and at the 5.10 MeV resonance

The spectra at these energies cannot be attributed to the pure direct three α decay nor to the pure sequential decay. The important fact is that at these energies two α decaying broad resonances closely overlap. In fact, as shown in Fig. 12, the differential cross section at $E_{23}=E_{31}$ and the differential cross section at $E_{23}=3$ MeV show peaks at different energies of the incident proton. The former represents mainly the intensity of the direct three α decay and has peaks at $E_p=2.6$ MeV, 3.7 MeV and 5.10 MeV. The latter represents the intensity of the sequential decay, and has peaks at about 2.4 MeV, about 3.6 MeV and about 4.95 MeV. Thus in Fig. 15, the α_1 and α_{11} peaks at the 5.10 MeV resonance come from the tail part of the 4.92 MeV resonance. The flat part is considered to come from the 5.10 MeV resonance.

As for spectra at $E_p=3.5$ MeV and $E_p=3.75$ MeV, a similar situation is expected. They show small peaks near the energies E_{α_1} and $E_{\alpha_{11}}$, and also show a fairly large yield in the flat part. Upper and lower slopes of spectra are complex. However, these features can be explained by simple summation of the spectra of the direct three α decay and that of the sequential decay. Besides, the energy dependence of spectra shows that the α_1 and α_{11} peaks become relatively larger at $E_p=3.5$ MeV, but the flat part becomes more dominant at 3.75 MeV. From these facts, it is considered that, of the overlapping two resonances the 3.75 MeV resonance contributes to the flat part and the 3.5 MeV resonance to α_1 and α_{11} peaks.

Consequently at the 3.75 MeV resonance and at the 5.10 MeV resonance the α decay can be considered to occur directly and at the 3.5 MeV resonance it can be considered to occur sequentially.

Thus, the data indicate that the decay mechanism at the resonances studied in the present work is either the direct-three-α-decay mechanism or the sequen-

tial decay mechanism. These results suggest that the decay mechanism reflects the structure of the compound state at the resonance. Especially for the direct three α decay, if the decaying state has a large α width, it is expected to have a simple three α structure. If the decaying state has a single particle structure, after emission of an α particle the residual nucleus will form ^{8}Be nucleus by some rearrangement process and then decays to two α particles. In this case, the decay mechanism is sequential. If it has a single α cluster structure, the process of the α decay will be possible like that of the single particle structure, but the probability of the α decay will be much larger. Even if it has an α-^{8}Be cluster structure, the decaying energy will not be statistically delivered to α particles, and the decay mechanism will be sequential. In the case of the sequential decay, the decaying state has a ^{8}Be cluster, or a more complicated structure and ^{8}Be* is formed in the decaying process.

In Fig. 16 are shown exciation functions reported by other authors for the outgoing channels induced by the (^{11}B+p) channel at the energy region of this work. In these excitation functions it is a remarkable feature that yields of

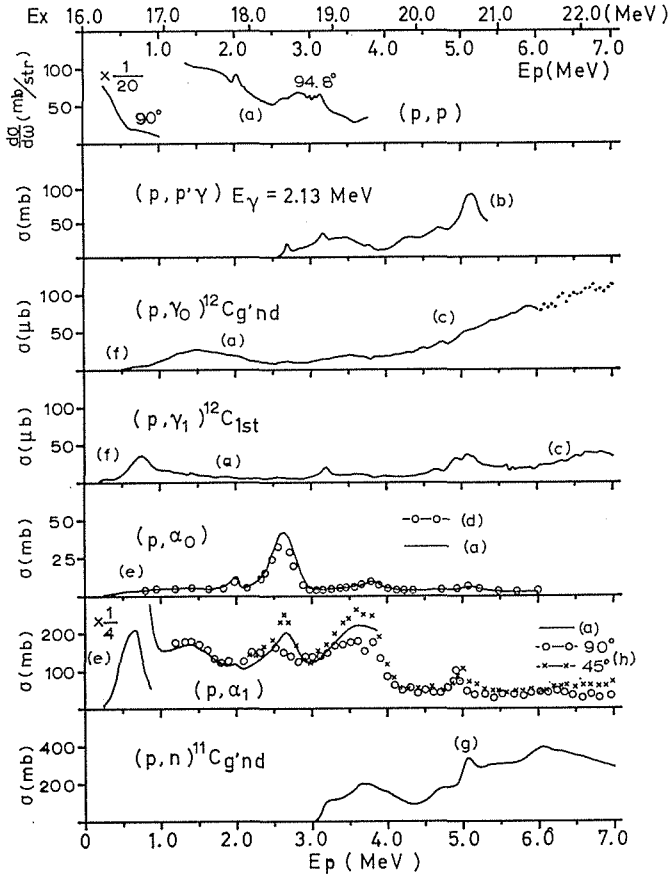

Fig. 16. Excitation functions of various reactions of the type ^{11}B(p, x)Y.
(a) ref. (26), (b) ref. (27), (c) ref. (28), (d) ref. (29), (e) ref. (30), (f) ref. (31), (g) ref. (32), and (h) differential cross section, ref. (33).

the α particle channels are strongly enhanced. The large reduced widths for the α decay of some levels, especially for the α_1 channel (including the direct three α decay) cannot be explained by the shell model with intermediate coupling.[34] This probably means that these levels have somewhat α cluster structures. Results in the present work seem to support the statement. Furthermore the existence of the resonance decaying directly to three α is very interesting in connection with the structures of the medium and higher excited states of light nuclei.[1,2,4]

However these levels are strongly excited through the proton channel and for some of these levels the isospin is assigned to be 1. If they have some sort of α cluster structures, probable clusters are appreciably diffused.

The most interesting level is the 18.36 MeV level. It shows large resonances in α channels but no resonance in gamma channels. The spin, parity and isospin are adsigned to be (3^-, T=0). Although R. E. Segal et al.[35] suggested the possibility of T=1 in connection with the 3.9 MeV level of ^{12}B, the strong resonances in the α channels and no resonance in the γ_1 channel[28] are considered to support the assignment of T=0. For this level the α decay show the direct three α decay mechanism, so the structure of this level is considered to be a three-α-cluster structure. Probably for the 19.4 MeV level (2^+, T=0), the same thing can be said.

6. Conclusion.

In the present experiments, energy dependences of coincident α energy spectra are measured to obtain information about α decay mechanisms and structures of the excited states of ^{12}C. Main features of the measurements are that energy dependence of spectra are obtained and that the selected detection conditions are much favourable to determine the decay machanism. In this condition, peaks of α_1 and α_{11} from the sequential decay are effectively separated without complexity of interference effects, and the statistical distribution of the direct three α decay is found in the region where all the relative energies are larger than about 3 MeV. From the qualitative discussion of the results, following conclusions are obtained.

i) At the 163 keV resonance (16.11 MeV in $^{12}C^*$; 2^+, T=1) and at the 2.62 MeV resonance (18.36 MeV; 3^-, T=0), spectra show the shape of the phase space volume over the region where all the relative energies of α particles are higher than about 3 MeV and quickly falling down outside the region. These spectra are considered to show the direct-three-α-decay mechanism.

ii) At about 215 keV, at about 2.4 MeV and at the 4.92 MeV resonance (20.47 MeV), spectra show the shape expected from the sequential decay mechanism. The positions and widths of the peaks well agree to those corresponding to the first excited state of ^8Be. These spectra are considered to show the sequential decay mechanism.

iii) At the 3.5 MeV resonance (19.2 MeV; 1^-, T=1), at the 3.75 MeV resonance (19.4 MeV; 2^+, T=0) and at the 5.10 MeV resonance (20.64 MeV; 3^-, T=1), spectra show more complicated shapes. However, they are considered to be superposition of the spectrum of the type i) and that of the type ii). Thus at the 3.5 MeV resonance, the decay mechanism is considered to be sequential. At the 3.75 MeV resonance and at the 5.10 MeV resonance, the

decay mechanism is considered to be direct.

iv) Structures of the states of ^{12}C which decay directly to three α particles are considered to be somewhat like the three α cluster structure. Of these states, the 18.36 MeV and probably the 19.4 MeV states are considered to have three α cluster structures, because they decay mainly to the α particle channel. Those states which decay sequentially are considered to have more complicated structures.

These conclusions are qualitative and derived from the results under limited detection conditions. The quantitative interpretation is desired which explains these results and others under different detection conditions. Moreover, as is suggested in this experiment, for the correct treatment of the three α decay it is necessary to investigate carefully various aspects of the decay in more details with experimental methods.

The three body decay mechanism has been scarecely used to investigate the nuclear structure. But results in this experiment show that it may be used as a tool to investigate the structure of the decaying state.

ACKNOWLEDGEMENT

The author is much indebted to Prof. J. Muto and Dr. K. Takimoto for many helpful suggestions, encouragements and cooperation.

He wishes to thank for interest and discussions to Prof. T. Yanabu and other members of the Cyclotron Laboratory, Institute for Chemical Research, Kyoto University. He is also grateful for stimulating discussion to Prof. K. Nishimura and other members of the Kyoto University tandem Van de Graaff Laboratory.

REFERENCES

1) G. C. Phillips and T. A. Tombrello; Nucl. Phys. 19 ('60) 555.
R. K. Sheline and K. Wildermuth; Nucl. Phys. 21 ('60) 196.
H. Morinaga; Phys. Rev. 101 ('56) 254.

2) K. Wildermuch and T. Kanellopoulos; Nucl. Phys. 7 ('58) 150.
L. D. Pearlstein, Y. C. Tang and K. Wildermuth; Nucl. Phys. 18 ('60) 23.
Y. C. Tang, F. C. Khanna, R. C. Herndon and K. Wildermuth; Nucl. Phys. 35 ('62) 421
G. C. Phillips and T. A. Tombrello; Nucl. Phys. 20 ('60) 648.
I. Shimodaya, R. Tamagaki and H. Tanaka; Progr. Theor. Phys. 27 ('62) 793.
J. Hiura and I. Shimodaya; Progr. Theor. Phys. 36 ('66) 977.
S. Saito, J. Hiura and H. Tanaka; Progr. Theor. Phys. 39 ('68) 635.
H. Horiuchi and K. Ikeda; Progr. Theor. Phys. 40 ('68) 277.

3) K. Takimoto; Memoires of the College of Science, University of Kyoto. Series A Vol. XXXI, No. 2, Article 12, 1967, Page 268.
T. Yanabu, S. Yamashita, K. Hosono, S. Matsuki, T. Tanabe, K. Takimoto, Y. Okuma, K. Ogino, S. Okuma and R. Ishiwari; Jour. Phy. Soc. Jap. 24 ('68) 667.
T. Yanabu, S. Yamashita, K. Takimoto and K. Ogino; Jour. Phys. Soc. Jap. 20 ('65) 1303.

4) A. I. Baz and V. I. Manko; Phys. Lett. 28B ('69) 541.
E. Almqvist, D. A. Bromley, J. A. Kuehner and B. Whalen; Phys. Rev. 130 ('63) 1140.

5) D. H. Wilkinson; Physica 22 ('59) 1039; Ann. Rev. Nucl. Sci 9 ('59) 1.

6) J. D. Anderson, C. Wong and J. W. McClure; Phys. Rev. 129 ('63) 2718.

7) A. M. Lane and R. G. Thomas, Rev. Mod. Phys. **30** ('58) 257.
8) F. Ajzenberg-Selove and T. Lauritsen; Nucl. Phys. 78 ('66) 1, and Nucl. Phys. **A114** ('68) 1.
9) E. H. Beckner, C. M. Jones and G. C. Pillips; Phys. Rev. **123** ('61) 255.
F. C. Barker and P. B. Treacy; Nucl. Phys. 38 ('62) 33.
C. Zupancic; Rev. Mod. Phys. **37** ('65) 330.
10) P. Swan; Rev. Mod. Phys. **37** ('65) 336.
11) D. Dehnhard, D. Kamke und P. Kramer; Ann. Phys. **14** ('64) 201.
D. Dehnhard; Rev. Mod. Phys. **37** ('65) 450.
12) D. Kamke und J. Krug; Zeit. Phys. **201** ('67) 301.
13) J. D. Bronson, W. D. Simpson, W. R. Jackson and G. C. Phillips; Nucl. Phy. 68 ('65) 241.
14) Y. S. Chen, S. T. Emerson, W. R. Jackson, W. D. Simpson and G. C. Phillips; Nucl. Phys. **A106** ('68) 1.
15) J. P. Longequeue, MMEN. Longequeue et H. Beaumevielle; Phys. Lett. **9** ('64) 171.
16) A. Giorini, D. Engelhardt, J. F. Cavaignac, J. P. Longequeue et R. Bouchez; Joul. Phys. **29** ('68) 4.
MM. Y. Flamant, Y. Chanut, F. Borardallah, R. Borardallah, R. Ballini et L. Marquez; Compt. Rend. Acad. Soc. Paris **264** ('67) B1283.
L. Marquez, J. P. Laugier, R. Ballini, C. Lemeille, N. Saunier et J. Rey; Nucl. Phys. **A97** ('67) 321.
17) L. Marquez; Thesis, Rapport CEA-R 3009.
J. L. Quebert and L. Marquez; Nucl. Phys. **A126** ('69) 646.
J. P. Laugier, M. Cadeau, G. Moulhayrat et L. Marquez; Joul. Phys. 29 ('68) 829.
K. Schäfer; Nucl. Phys. **A140** ('70) 9.
P. M. Cockburn, L. J. B. Goldfarb, I. S. Grant and H. E. Reed; Nucl. Phys. **A141** ('70) 532.
A. Giorni; Nucl. Phys. **A144** ('70) 146.
18) L. M. Delves; Nucl. Phys. **9** ('58) 391.
F. T. Smith; Phys. Rev. **120** ('60) 1058.
A. T. Dragt; Jour. Math. Phys. **6** ('65) 533.
19) D. Dehnhard, D. Kamke und P. Kramer; Phys. Lett. **3** ('62) 52.
P. Kramer; Rev. Mod. Phys. **37** ('65) 346.
W. Zickendraht; Zeit. Phys. 200 ('67) 194.
20) G. C. Phillips, T. A. Griffy and L. C. Biednharn; Nucl. Phys. **21** ('60) 327.
21) G. C. Phillips; Rev. Mod. Phys. **36** ('64) 1085.
G. C. Phillips; Rev. Mod. Phys. **37** ('65). 409.
22) G. G. Ohlsen; Nucl. Instr. Meth. **37** ('65) 240.
23) K. M. Watson; Phys. Rev. 88 ('52) 1163.
24) J. Lang, G. Muller, W. Wolfli, R. Bosch and P. Marmier; Phys. Lett. **15** ('65) 248.
C. Kacser and T. J. Aitchson; Rev. Mod. Phys. **37** ('65) 350.
25) T. Sidei, et al.; Memoirs of the Faculty of Science, KUVL-1.
26) R. E. Segel, S. S. Hanna and R. G. Allas; Phys. Rev. **139** ('65) B818.
27) J. K. Bair, J. D. Kington and H. R. Willard; Phys. Rev. **100** ('55) 21.
28) R. G. Allas, S. S. Hanna, L. Meyer-Schutzmeister and R. E. Segel; Nucl. Phys. 58 ('64) 122.
29) G. D. Symons and P. B. Treacy; Nucl. Phys. **46** ('63) 93.
30) Q. Beckman, T. Huus and C. Zupancic; Phys. Rev. **91** ('53) 606.
31) J. Huus and R. B. Day; Rev. **91** ('53) 597.
32) J. C. Qverley and R. R. Borchers; Nucl. Phys. **65** ('65) 156.
33) J. Muto, K. Takimoto and I. Yamane; to be published.
34) V. V. Balashov and J. Rotter; Nucl. Phys. **61** ('65) 138.
35) F. P. Mooring, J. E. Monahan and R. E. Segel; Phys. Rev. 178 ('69) 1612.